Article ID: 1000-7032(2010)01-0079-07

Structural Design of Vertical-external-cavity Surface-emitting Semiconductor Laser with 920 nm

LIANG Xue-mei[1], LU Jin-kai[3], CHENG Li-wen[1], QIN Li[1], NING Yong-qiang[1], WANG Li-jun[1*]

(1. *Changchun Institute of Optics, Fine Mechanics and Physics, Chinese Academy of Sciences Changchun* 130033, *China*;
2. *Graduate School of Chinese Academy of Sciences, Beijing* 100049, *China*;
3. *Aviation University of Air Force, Changchun* 130022, *China*)

Abstract: A vertical-external-cavity surface-emitting 920 nm semiconductor laser (OP-VECSEL) with active region of $In_{0.09}Ga_{0.91}As$ quantum well (QW) system pumped by 808 nm laser diode module was constructed and optimized. By the finite element method, self-consistent solutions of electronic and optical equations of the semiconductor laser were realized and the characteristic parameters of OP-VECSEL were calculated. The performances of the especial mode in device, the threshold and the optical-optical conversion efficiency were analyzed by dealing with different structure parameters, including number of QWs (1, 2 and 3) in one period, QW depth, width and component of barrier and dimension of the non-absorption layer. The best structure of the laser was chosen.

Key words: semiconductor lasers; structural design; finite element; vertical external-cavity surface emitting laser; optically pumped

CLC number: TN248.4 **PACS:** 42.55.Px **PACC:** 4255P **Document code:** A

1 Introduction

High-power blue laser is of commercial interest in laser projection display. Historically, blue laser has been provided by either Ar-ion lasers or diode pumped solid state lasers. However, these gas or solid state lasers are expensive in both purchasing and operating, difficult to be maintained, inefficient and relatively bulky to be applicable to consumer electronics. As laser projection display technologies have been explored for very long time, there are several matured image processing technologies, such as GEMS, GLV, and DLP. However commercially cheap visible laser sources are still under development and have acted as a limiting factor in laser projection display.

High-power, high-brightness lasers are the key for a wide range of commercial and defense applications. OPS-VECSELs have particularly become attractive for their high power and excellent beam quality [1-6]. They can be used in a wide range of applications including fiber laser pump source, intracavity frequency doubling, mode-locking [7], tuning of the wavelength [8], radar and free space communication. In these lasers, a semiconductor multi-quantum wells active region and a distributed Bragg reflector (DBR) stack with a thick of a few microns, are mounted on the heat spreader or heat sink, resulting in efficient heat dissipation which makes VECSEL become a strong candidate in power-scalable lasers [2,3].

Received date: 2009-08-25; **Revised date:** 2009-10-15

Foundation item: Project supported by the National Science Foundation of China under Contract Number NSFC(60636020, 60676034, 60706007); Project supported by CAS Innovation Program; National Science Foundation of Jilin Province (20080335, 20086011)

Biography: LIANG Xue-mei, female, born in 1982, Jilin Province. Her work focus on designing semiconductor lasers and correlative experiment.
E-mail: liangxuemei1026@hotmail.com, Tel: (0431)86176335
* : Corresponding Author; E-mail: wanglj@ciomp.ac.cn, Tel/Fax: (0431)84627013

Optical pumping of multi-quantum wells is the most straightforward way to achieve a uniform carrier distribution over a large pump area, and is particularly advantageous for multi-watt operation. The external output coupler (mirror) and pump spot (aperture) leads to transverse mode operation. These lasers are relatively insensitive to the pump wavelength variation, making the overall package become low cost and simple. Recently, VECSEL combined with intra-cavity frequency doubling has been emerged as a promising solution to provide visible light sources for display [6]. Chilla and his collogues reported high-power green and blue VECSELs. However, the optical threshold power for the 460 nm laser is higher than that of 530 nm laser [6] and even higher than that of 488 nm laser [7]. Since the frequency doubling efficiency for the 460 nm is intrinsically higher than those of longer wavelength lasers due to its higher energy, the higher threshold power of 460 nm may be mainly cased by its lower optical efficiency of 920 nm VECSEL. Therefore, we should analyze and optimize the structure of high efficiency 920 nm OPS-VECSEL.

Because of microcosmic dimension, complex operation mechanism of semiconductor lasers, and many factors of affecting device performance, using of computer assistant design is much better than use a simple model to demonstrate out their characteristics [10]. The structures of OPS-VECSEL are comparatively complex, whose characteristics are affected by lots of factors, and consequently analyzing their structures and physics characteristics is needed to anatomize for enhancing their output performance. The device performances were calculated according to these basic equations that can describe the electrical and optical behaviors of the semiconductor lasers [4].

2 Theoretical Model

2.1 VECSEL Description

For a conventional VECSEL system, the VECSEL structures include a bottom DBR and a resonant periodic gain structure (RPG) with InGaAs QWs. The surface of the structure finishes with a window layer. The structures were grown by MOCVD on GaAs substrate. InGaAs quantum well (QW) and GaAs barrier structure form an active layer pumped by the high-power laser diode module at around 808 nm. The RPG structure consists of GaAs barriers (as a pump laser absorbing layer), 4 ~ 20 periods InGaAs single QW positioned at the antinodes of standing wave, spaced by half wavelength with strain compensation GaAsP layers. The DBR has 17 ~ 27 pairs of $Al_{0.2}Ga_{0.8}As/AlAs$ stacks. The window layer consists of $Al_{0.3}Ga_{0.7}As$ to prevent carrier recombination at surface and thin GaAs to prevent surface oxidation. Pump light power is greater than 5 W, the reflectivity of external cavity mirror is between 87% and 99%.

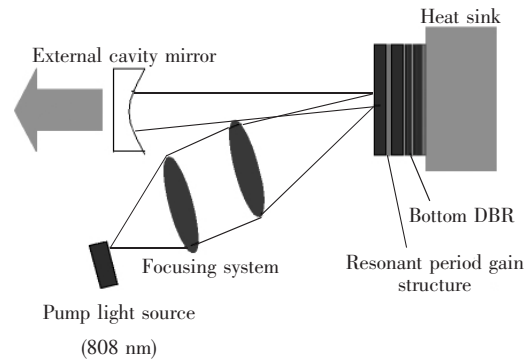

Fig. 1 Structural sketch of OPS-VCSEL

2.2 Theoretical Analysis

The basic equations used to describe the electrical behavior of the semiconductor device are Poisson's equation

$$\nabla \cdot (\varepsilon \nabla V) = -q(p - n + N_D - N_A), \quad (1)$$

and the current continuity equations for electrons and holes are

$$\nabla \cdot J_n = q(R - G), \quad (2)$$

$$\nabla \cdot J_P = q(R - G), \quad (3)$$

ε is the medium dielectric constant interrelated with the vacuum, V is the electrostatic potential, q is the electric charge, n and p are the electron and hole concentrations, respectively, N_D and N_A are separately the ionized donor and acceptor concentrations, J_n and J_p are the electron and hole carrier flux densities. The equations (2) and (3) are independent of the time, R and G are the static recombination and generation rate, respectively.

The wave equation and the photon rate equation are used to describe the optical behavior. The wave equation of TE mode is

$$\left[\frac{\partial^2}{\partial x^2} + \varepsilon k_0^2 - \beta^2\right] \cdot E = 0, \quad (4)$$

$k_0 = 2\pi/\lambda_0$ (λ_0 is the emitting wavelength), β is the mode propagation constant, E is the optical field. In the equilibrium condition, the photon rate equation could be written as

$$\frac{\mathrm{d}S}{\mathrm{d}t} = R_{\mathrm{st}}S + \frac{N}{\tau_{\mathrm{r}}} - \frac{S}{\tau_{\mathrm{p}}}, \quad (5)$$

S is photon density of single mode, R_{st} is stimulated emission rate, N is electron concentration, τ_{r} is spontaneous emission recombination lifetime of the electron, τ_{p} is photon lifetime [11].

To depict the entire behavior of the lasers, the mode output power is an important parameter.

$$P = \frac{1}{2}\frac{c^2}{\bar{n} \cdot \lambda} h \frac{1}{L} \ln\left(\frac{1}{R_1 R_2}\right) \cdot \sum N_{\mathrm{p}}, \quad (6)$$

$\bar{n}$ is the material refractive index of the active region, L is the laser cavity length, R_1 and R_2 are reflectivity of the DBR and external cavity mirror, N_{p} is the photon amount in the cavity of the mode p.

Using the finite element analysis through these above basic electrical and optical equations, we built a calculation module for the OPS-VECSEL. By building up the material storage and setting optical power density, center wavelength, threshold, scan step size and calculation precision, the output characteristics of these devices were calculated.

The performances of device especially the mode, the threshold and the optical-optical conversion efficiency were analyzed by dealing with different number of QWs (1, 2 and 3) in one period, QW depth, barrier width, the component and dimension of the non-absorption layer. Base on these results, optimization could be done according to the practical application.

3　Results and Discussion

Usually, it is very crucial for VECSEL that the RPG structure must only include one single QW to accurately match the antinode positions of standing wave. Ongstad *et al*. studied on carrier recombination of InGaAs QWs with various potential depths and reported that the saturated carrier lifetime in the shallow QW is much longer than that of deep QW at high injection level [12]. In our case, as the pump power level is very high, the carrier lifetime is easily saturated and due to the longer saturated carrier lifetime in 920 nm QW, some of excited carrier in the (especially middle of) GaAs barrier cannot diffuse into the QW and tends to recombine in the GaAs barriers. For the sake of decreasing carrier nonradiative recombination rate, the conventional VECSEL structure was ameliorated. By increasing the number of QW from 1 to 3 the quantum status increase and thereby the saturated carrier lifetime decreases. Fig. 2 shows mode characteristics of different number of quantum well. As the number of QW increased from 1, 2 to 3, the oscillation of the main model could be enhanced, while others' should be depressed. Accordingly, 3 QWs RPG structure had been chosen.

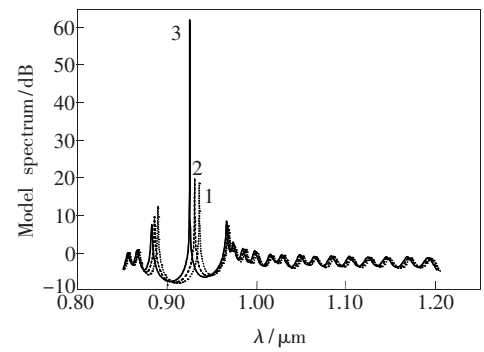

Fig. 2　Model characteristics of different number of quantum well

Output characteristics with different quantum well depth were shown in Fig. 3(a) ~ (c). The QW structure for curve 1 is $In_{0.09}Ga_{0.91}As/GaAs_{0.9}P_{0.1}/GaAs$, for curve 2 it is $In_{0.09}Ga_{0.91}As/GaAs/GaAs_{0.9}P_{0.1}$. Fig. 3 (a) shows incident power and output power with different quantum well depth. Compare with curve 1, threshold of curve 2 decreased from 0.21×10^9 to 0.20×10^9 W/m^2, optical-optical conversion efficiency of curve 2 increases. Mode characteristics with different quantum well depth are shown in Fig. 3 (b). The oscillation of the main model of curve 2 enhances from 28.4 dB to 38.6 dB. Fig. 3(c) showes conductive bands of

different quantum well depth. The quantum well depth of structure 1 and 2 were calculated, which are 0.19 eV and 0.24 eV, respectively. Consequently, $In_{0.09}Ga_{0.91}As/GaAs/GaAs_{0.9}P_{0.1}$ structure is chosen.

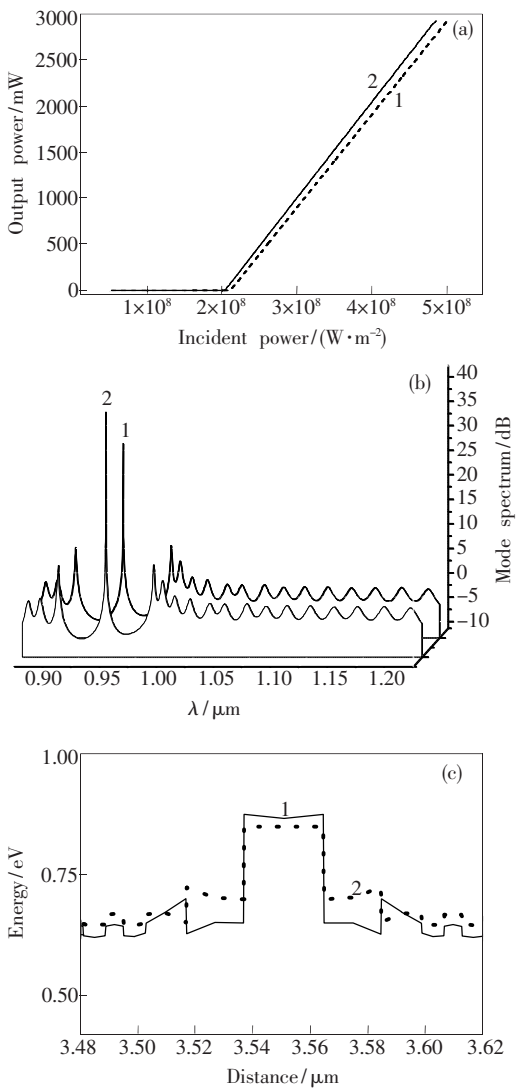

Fig. 3 (a) Incident power and output power with different quantum well depth; (b) Mode characteristics with different quantum well depth; (c) Conductive bands of different quantum well depth.

Output characteristics with different barrier width are shown in Fig. 4 (a) and Fig. 4 (b). 4 curves expresse 4 different structures, each RPG has 3 QWs. The width of QW $In_{0.09}Ga_{0.91}As$ is 8 nm, but the barriers´ width are different. The structure of curve 1 and 2 is shown in Fig. 7. The width of 2 barriers in the middle is 6 nm, which are sandwiched between 2 barriers whose width is 14 nm. The structure of curve 3 and 4 have 4 barriers with width of 10 nm. The QW structure for curve 1 and 3 is $In_{0.09}Ga_{0.91}As/GaAs_{0.9}P_{0.1}/GaAs$, for curve 2 and 4 it is $In_{0.09}Ga_{0.91}As/GaAs/GaAs_{0.9}P_{0.1}$. It is obvious in Fig. 4 (a) that threshold of curve 1 and 2 is much lower, while optical-optical conversion efficiency is much higher, thus, barrier width can affecte device performance quietly. Fig. 4 (a) also showes that for the structure having same barrier width, threshold and optical-optical conversion efficiency almost have no change when the barrier material changed. The most oscillation of the main model of these 4 curves is curve 2 as shown in Fig. 4 (b). Hence, this structure should be chosen that the width of 2 barriers in the middle is 6 nm, which are sandwiched between 2 barriers with width of 14 nm, the QW is $In_{0.09}Ga_{0.91}As/GaAs/GaAs_{0.9}P_{0.1}$.

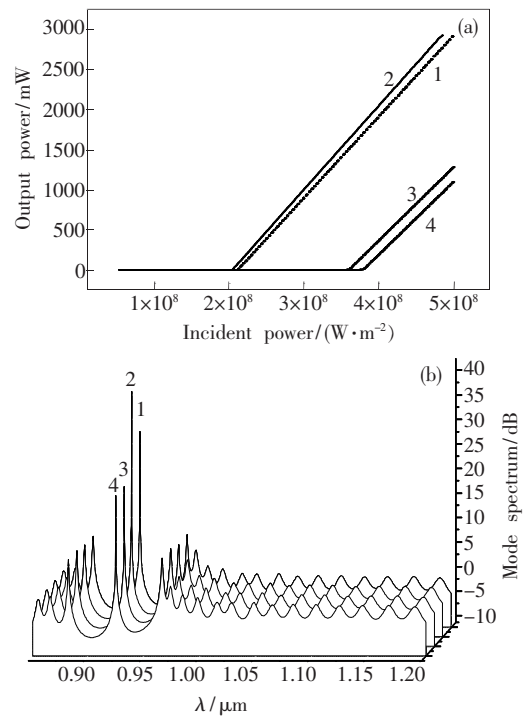

Fig. 4 (a) Incident power and output power with different barrier width; (b) Mode characteristics of different barrier width.

The pump power level is very high which will easily cause the carrier hot overflowed. So, an AlGaAs non-absorbtion layer is inserted in the middle of GaAs barriers to prevent the carrier hot overflowed. Fig. 5 (a) and Fig. 5 (b) show the output characteristics with different non-absorption layer

component. The non-absorbtion layer of curve 1, 2 and 3 are $Al_{0.2}Ga_{0.8}As$, $Al_{0.3}Ga_{0.7}As$ and $Al_{0.4}Ga_{0.6}As$, respectively. As the Al component increased, the optical-optical conversion efficiency is reduced, while threshold nearly has no change, and the oscillation of the main model is enhanced. Taking these factors into account, $Al_{0.3}Ga_{0.7}As$ is selected as non-absorbtion layer.

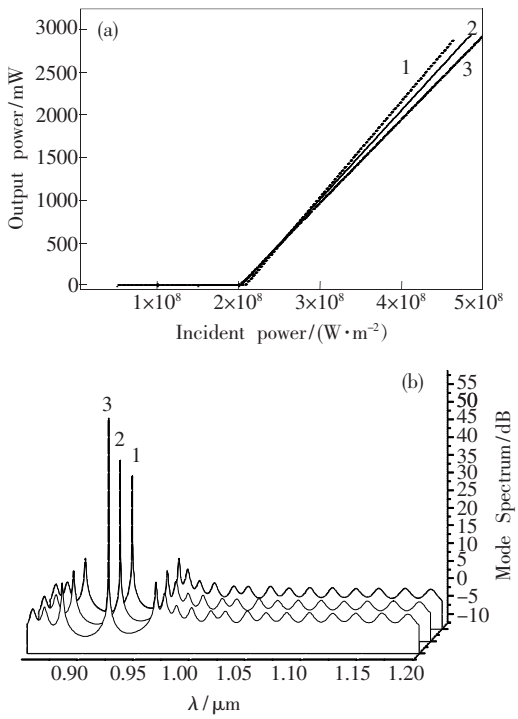

Fig. 5　(a) Incident power and output power with different non-absorption layer component; (b) Mode characteristics of different non-absorption layer component.

Output characteristics with different non-absorption layer dimension are shown in Fig. 6(a) and Fig. 6(b). Three kind of $Al_{0.3}Ga_{0.7}As$ non-absorbtion layer were attempted, 18 nm, 28 nm and 38 nm are separately corresponding to curve 1, 2 and 3. As the non-absorption layer dimension increased, the optical-optical conversion efficiency is reduced, while threshold nearly has no change, and the oscillation of the main model is weaken. The non-absorption layer dimension hereby is taken 18 nm for choice.

Base on the theoretical calculation results, we chose the optimized structure of them. There are three $In_{0.09}Ga_{0.91}As/GaAs/GaAs_{0.9}P_{0.1}$ QWs in this structure, as shown in Fig. 7, $In_{0.09}Ga_{0.91}As$ is well, GaAs is barrier, $GaAs_{0.9}P_{0.1}$ is strain compensation layer, $Al_{0.3}Ga_{0.7}As$ is non-absorbtion layer. The width of 2 barriers in the middle is 6 nm, which are

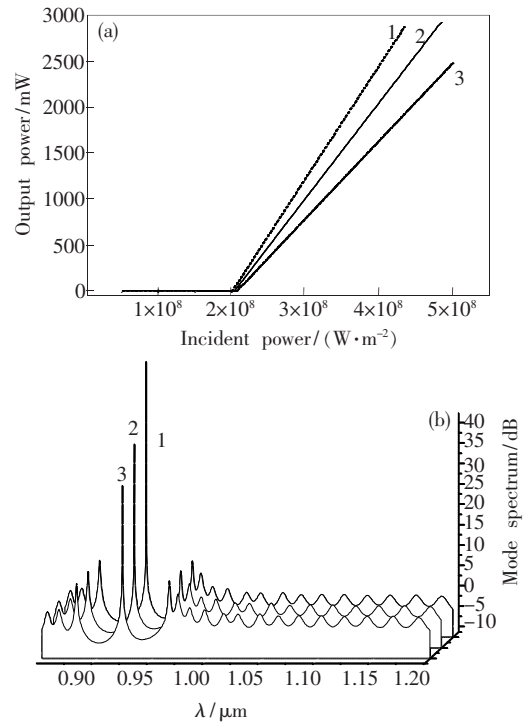

Fig. 6　(a) Incident power and output power with different non-absorption layer dimension; (b) Mode characteristics of different non-absorption layer dimension.

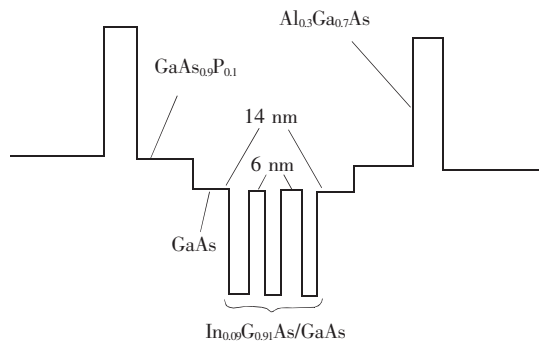

Fig. 7　The optimized conduction band diagram

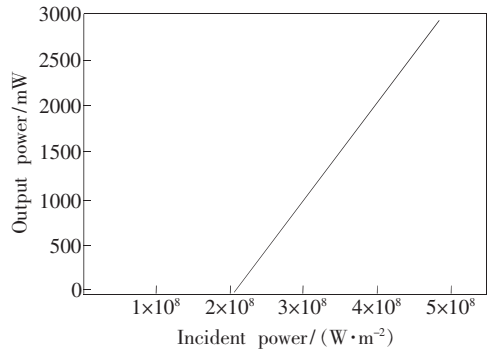

Fig. 8　Incident power and output power of the optimized structure

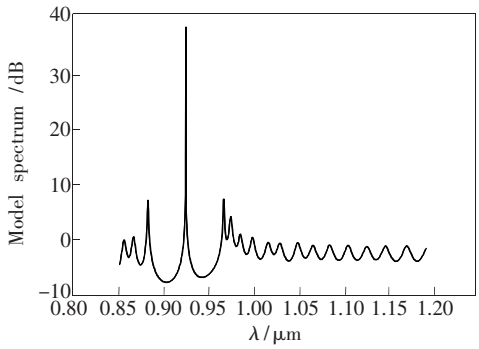

Fig. 9 Mode characteristics of the optimized structure

sandwiched between 2 barriers whose width is 14 nm. Output characteristics of the optimized one is shown in Fig. 8 and Fig. 9.

4 Conclusion

In this paper, we constructed and optimized a 920 nm OPS-VECSEL with active region of $In_{0.09}Ga_{0.91}As$ QW system pumped by 808 nm laser diode module. The number of QW is increased from single to triple to increase the quantum states and thereby decrease the saturated carrier lifetime. We optimized QW structure from $In_{0.09}Ga_{0.91}As/GaAs_{0.9}P_{0.1}$ to $In_{0.09}Ga_{0.91}As/GaAs/GaAs_{0.9}P_{0.1}$, thereinto, GaAs is barrier layer, $GaAs_{0.9}P_{0.1}$ is strain compensation layer. The width of two barriers layer in the middle is 6 nm, which are sandwiched between two barriers whose width is 14 nm. This amelioration can reduce threshold value. We inserte an $Al_{0.3}Ga_{0.7}As$ non-absorbtion layer in the middle of $GaAs_{0.9}P_{0.1}$ strain compensation layers, not to generate excessive carriers which tend, to recombine in the GaAs barriers. The $Al_{0.3}Ga_{0.7}As$ layer were also expected to act as a diffusion barrier which prevents carriers from diffusion to the longer direction. Correlative experiments will be presented in another paper.

References:

[1] Kuznestov M, Harkimi F, Sprague A R, *et al*. Design and characteristics of high-power (>0.5-W CW) diode-pumped vertical-external-cavity surface-emitting semiconductor lasers with circular TEM_{00} beams [J]. *IEEE J. Sel. Top. Quantum Electron.*, 1999, **5**(3):561-573.

[2] Chillar J, Butterworth S, Zeitschel A, *et al*. High power optically pumped semiconductor lasers [J]. *SPIE*, 2004, **5332**: 143-150.

[3] Fan L, Fallahi M, Hader J, *et al*. Over 3 W high-efficiency vertical-external-cavity surface-emitting lasers and application as efficient fiber laser pump sources [J]. *Appl. Phys. Lett.*, 2005, **86**(21):211116-1-3.

[4] Cheng Liwen Liang Xuemei, Qin Li, *et al*. Theoretical analysis of key parameters of 980 nm optically pumped semiconductor vertical external cavity surface emitting laser [J]. *Chin. J. Lumin.* (**发光学报**), 2008, **29**(4):713-715 (in Chinese).

[5] Peng Biao, Ning Yongqiang, Qin Li, *et al*. Polarization characteristics of 980 nm high power vertical cavity surface emitting laser [J]. *Chin. J. Lumin.* (**发光学报**), 2008, **29**(5):845-850 (in Chinese).

[6] Ma Qiang, Tian Zhenhua, Wang Zhenfu, *et al*. A theoretical model of high power VCSEL based on the thermal-offset-current [J]. *Chin. J. Lumin.* (**发光学报**), 2009, **30**(4):463-466 (in Chinese).

[7] Aschwanden A, Lorenser D, Unold H J, *et al*. 10 GHz passively mode-locked external-cavity semiconductor laser with 1.4 W average output power [J]. *Appl. Phys. Lett.*, 2005, **86**(13):131102-1-3.

[8] Hastie J, Calvez S, Dawson M D. High power CW red VECSEL with linearly polarized TEM_{00} output beam [J]. *Optics Exp.*, 2005, **13**(1):77-81.

[9] Chillar J L A, Zhou H, Weiss E, *et al*. Blue and green optically-pumped semiconductor lasers for display [J]. *SPIE*, 2005, **5740**:41-47.

[10] Chen Weiyou, Zhang Yejin, Liu Shiyong. *Computer Aided Design and Analysis of Semiconductor Laser* [M]. Changchun: Publishing House of Jilin University, 2003, 1-10 (in Chinese).

[11] Jiang Jianping. *Semiconductor Laser* [M]. Beijing: Publishing House of Electronics Industry, 2000, 109-110 (in Chinese).

[12] Ongstad A P, Gallant D J, Dente G C. Carrier lifetime saturation in InGaAs single quantum wells [J]. *Appl. Phys. Lett.*, 1995, **66**(20):2730-2732.

920 nm 光抽运垂直外腔面发射半导体激光器结构设计

梁雪梅[1,2]，吕金锴[3]，程立文[1,2]，秦　莉[1]，宁永强[1]，王立军[1*]

（1. 中国科学院 长春光学精密机械与物理研究所，吉林 长春　130033；
2. 中国科学院 研究生院，北京　100049；　3. 空军航空大学，吉林 长春　130022）

摘要： 设计并优化了一种用 808 nm 的大功率激光二极管为抽运光源，$In_{0.09}Ga_{0.91}As$ 量子阱结构为增益介质的 920 nm 光抽运半导体垂直外腔面发射激光器。运用有限元方法，对激光器的电特性方程和光特性方程求自洽解，计算了器件各种特性参量。分析了单个周期内不同阱的个数（1，2 和 3）、不同阱深、不同垒宽、不同非吸收层组分、不同非吸收层尺寸条件下，器件性能的改变，特别是模式、阈值和光-光转换效率的改变，从而选择一个最佳的结构。

关　键　词： 半导体激光器；结构设计；有限元；垂直外腔面发射激光器；光抽运
中图分类号： TN248.4　　**PACS：** 42.55.Px　　**PACC：** 4255P　　**文献标识码：** A
文章编号： 1000-7032(2010)01-0079-07

收稿日期： 2009-08-25；**修订日期：** 2009-10-15
基金项目： 中国科学院知识创新工程领域前沿项目；国家自然科学基金(60636020，60676034，60706007)；吉林省科技发展计划(20080335，20086011)资助项目
作者简介： 梁雪梅(1982－)，女，吉林长春人，博士研究生，主要从事半导体激光器件的设计与实验工作。
E-mail：liangxuemei1026@hotmail.com，Tel：(0431)86176335
*：通讯联系人；E-mail：wanglj@ciomp.ac.cn，Tel/Fax：(0431)84627013